Baghdad Science Journal

Volume 22 | Issue 6 Article 6

6-17-2025

Utilizing an Atomic Force Microscopy with Continuous Flow Injection Analysis using NAG-4(sources)x3 with Three Solar Cells (NAG-4SX3-3D) Analyzer for Studying the Surface Morphology of the Precipitate of the Cyproheptadine-HCl and Loratadine

Bakr Sadiq Mohammed
Department of Chemistry, College of Science, University of Baghdad, Baghdad, Iraq,
bakralalazaw98@gmail.com

Nagham Shakir Turkey
Department of Chemistry, College of Science, University of Baghdad, Baghdad, Iraq,
nagamturkey@yahoo.com

How to Cite this Article

Mohammed, Bakr Sadiq and Turkey, Nagham Shakir (2025) "Utilizing an Atomic Force Microscopy with Continuous Flow Injection Analysis using NAG-4(sources)x3 with Three Solar Cells (NAG-4SX3-3D) Analyzer for Studying the Surface Morphology of the Precipitate of the Cyproheptadine-HCl and Loratadine," *Baghdad Science Journal*: Vol. 22: Iss. 6, Article 6.
DOI: https://doi.org/10.21123/2411-7986.4956

BAGHDAD SCIENCE JOURNAL 2025;22(6):1801–1814

Scan the QR to view the full-text article on the journal website

RESEARCH ARTICLE

Utilizing an Atomic Force Microscopy with Continuous Flow Injection Analysis using NAG-4(sources)x3 with Three Solar Cells (NAG-4SX3-3D) Analyzer for Studying the Surface Morphology of the Precipitate of the Cyproheptadine-HCl and Loratadine

Bakr Sadiq Mohammed *, **Nagham Shakir Turkey**

Department of Chemistry, College of Science, University of Baghdad, Baghdad, Iraq

ABSTRACT

The objective of this study is to describe surface morphology using Continuous Flow Injection Analysis CFIA, Atomic Force Microscopy AFM, and the homemade NAG-4(sources)x3 with three solar cell Analyzer NAG-4SX3-3D analyzer. Using a novel method for determining both drugs via reaction of both drugs, the study aims to determine the roughness parameters of (white precipitate of loratadine with sodium nitroprusside and yellow precipitate of cyproheptadine hydrochloride with 3,5-dinitro salicylic acid) for the AFM sample. The main advantage of the proposed technique is its ability to compute the amount of nanoparticles that can fill the empty surface area. Starting with the first ground, the monolayer calculates the free surface area and determines the concentration of the participating nanoparticles on the surface. A microfluidic flow system is thus proposed to produce nanoparticles on a continuous basis by means of a chemical reaction between precipitation reagents and medicinal active ingredients. The flow mechanism allows for the smooth and clog-free synthesis of the nanoparticles. Each and every chemical and physical flow injection conditions were examined and fixed. The average diameters of cyproheptadine hydrochloride for the surface area of a scanned section with dimensions of 20529961 nm^2 and 1.6601 $\times$ 10^{-15} nmol/grain are 96.73 nm, Grain No. 547, surface area of a single granule 29380.015706 nm^2, and number of layers 4; for loratadine, the average diameters are 88.87 nm, Grain No. 434, surface area of a single granule 24799.333466 nm^2, and number of layers 1 for the scanned section whose dimensions are 10762910.72 nm^2 and 1.3804 $\times$ 10^{-12} nmol/grain.

Keywords: Atomic force microscopy, NAG-4SX3-3D analyzer, Continuous flow injection analysis, Cyproheptadine hydrochloride, Loratadine

Introduction

The continuous flow injection analysis (CFIA) fast technique is an easy, simple, and versatile method in chemical analysis. It is considered one of the methods used to automate other methods; it depends on the chemical and physical factors of a scattered specimen region, from the blueness of the specimen inside the carrier stream and revealing.[1] Continuous flow processing is now widely accepted as a disruptive technology in the synthesis of active pharmaceutical ingredients (APIs) as well as other fine and commodity chemicals. This processing method has proven particularly useful in multiple synthetic transformations in sequence, known as multistep flow synthesis. This approach has been utilized to

Received 22 January 2024; revised 29 March 2024; accepted 31 March 2024.
Available online 17 June 2025

* Corresponding author.
E-mail addresses: bakralalazaw98@gmail.com (B. Sadiq Mohammed), nagamturkey@yahoo.com (N. Shakir Turkey).

https://doi.org/10.21123/2411-7986.4956

synthesize a number of APIs, often providing significant improvements in processing time, safety and yield.[2] Loratadine is often used for many applications. The primary applications of loratadine include: allergic rhinitis therapy, hay fever treatment, alleviating sneezing and mitigating inflammation in the eyes and nose, a very efficient remedy for skin allergies, such as urticaria.[3] Cyproheptadine hydrochloride $C_{21}H_{12}N.HCl$ has antihistamine and anti-serotonergic effects. Cyproheptadine hydrochloride is a solid that is crystallized and has a molecular weight of 350.9. It can be white or barely yellow. The chemical is soluble in water, methanol, and chloroform, but it's not very soluble in ethanol. Cyproheptadine often causes side effects like increased hunger, weight gain, depression, and sleepiness.[4,5] The most well-known and conceptually the straightest forward of the three force spectroscopy methods discussed in this article is atomic force microscopy (AFM).[6,7] The scanning tunneling microscope's inability to image nonconductive materials led to the development of the atomic force microscope. The primary function of an atomic force microscope is imaging, but it can also measure intra- and intermolecular interaction forces with resolution as small as one piconewton. This particular kind of atomic force microscope is known as a molecular force probe (MFP) when it is used for one-dimensional force measurements.[8] The cantilever, or small spring, is carried by the support of the AFM. It is oscillated by a ceramic piezoelectric material. A sharp probe, or tip, is fixed to the free end of the cantilever. The detector records the cantilever's motion and deflection, as shown in Fig. 1. On top of the sample specimen is the sample. As the cantilever approaches the surface of the sample and approaches in close proximity, a repulsive force progressively gains control and induces it to deviate from the surface.[9] One of the consequences is that a new set of artefacts might arise in the picture, which consumers used to traditional microscopy may not recognize.[10] Sources of artefact in AFM images include vibrations, the feedback circuit, the tip, the scanner, and the image processing software. In this paper a developed method is described to determine of cyproheptadine hydrochloride and loratadine using continuous flow injection-NAG-4SX3-3D coupled with AFM and aims to know the homogeneous distribution of the active substance during the manufacture of pills, study the sizes of crystals formed within the precipitate, and calculate the surface area of the active substance.

Tip artifacts

The AFM images obtained with a tip will always be impacted by its geometric form. It should go without saying that the profile will closely match its genuine form if the tip is much sharper than the feature being seen. The tip's sidewall angle and apex sharpness will both matter, depending on the height and lateral dimensions of the subject that has to be photographed. Generally speaking, the lateral geometry of objects exhibits the most artefacts, whereas the height of the features is correctly copied and unaffected by the tip form.[11] The Atomic Force Microscope concept is shown in Fig. 1. The forces exerted on a sample and a fine tip is measured by the AFM. The tip of a cantilever is brought very close to a surface and fastened to its free end. The cantilever will bend either positively or negatively due to repulsive or attractive forces that occur due to interactions between the tip and the surface. A laser beam that is reflected from the cantilever's backside is used to detect the bending.[12]

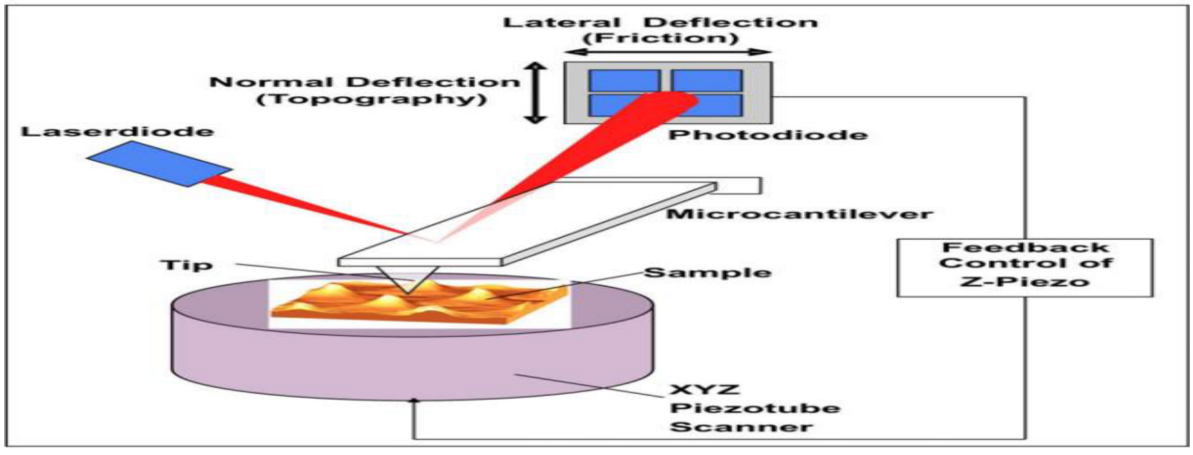

Fig. 1. A typical AFM setup with 3-D nanoscale interaction forces on the AFM probe tip, where these forces vertically bend and laterally twist the probe for topography.

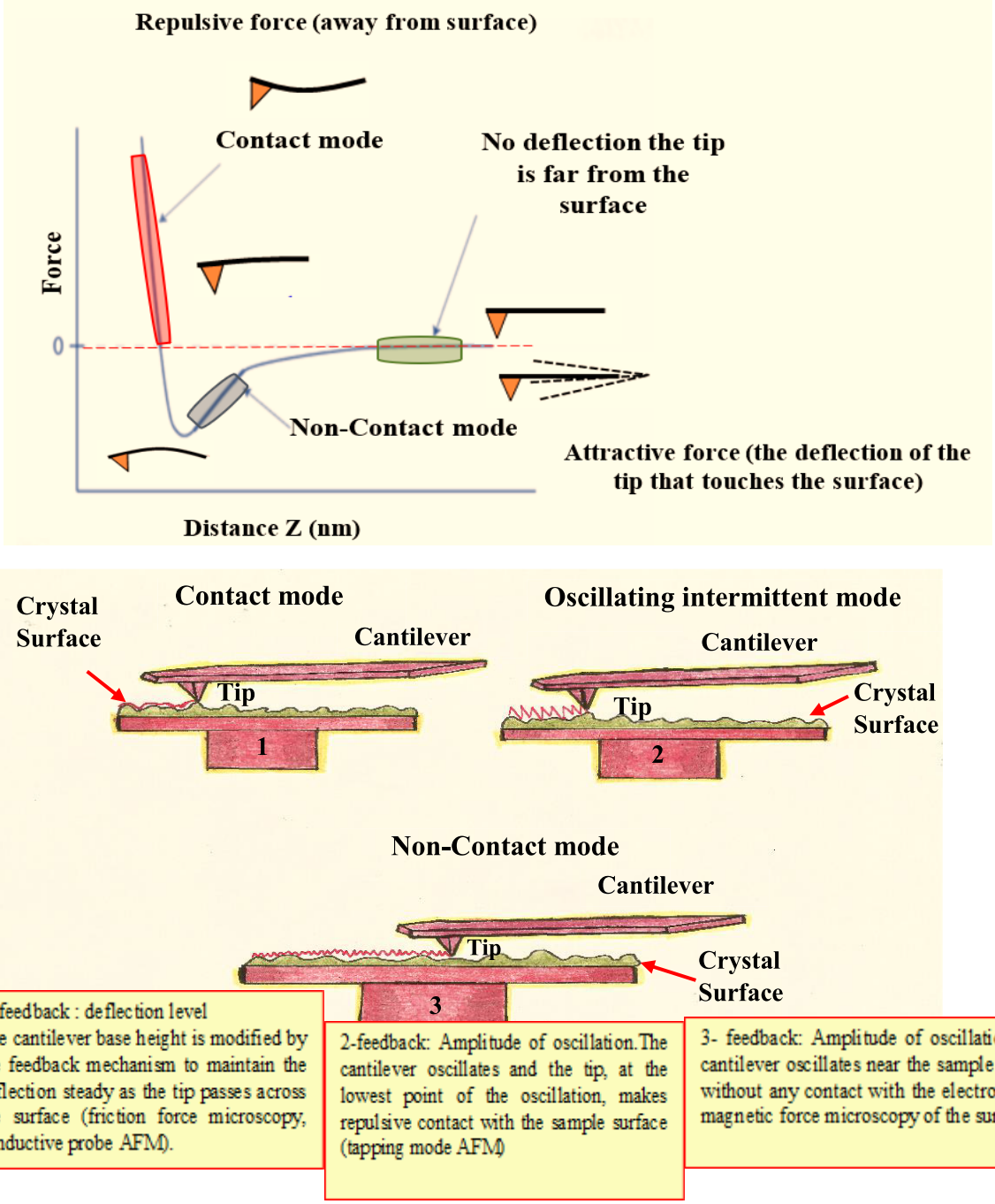

Fig. 2. Mechanism of cantilever works, piezoelectric property & tip – sample separation.

Piezoelectric property[13] is employed to generate alternative modes of conduct that will be addressed. The attraction and repulsion forces that are created while mapping the topography for a precipitate surface are seen in Fig. 2. It also displays three different modes of operation (i.e., when the probe tip makes contact with the sample surface, it is in contact mode; when it does not really touch the surface, it is in non-contact mode; and when the tip oscillates above the sample, it is in oscillating intermittent mode).

AFM has been used to determination many samples.[14–17] As well as, many techniques have been used coupled with AFM to determination of many samples such as: CFIA-AFM,[18] XRF,[19,20] NAG-4SX3-3D-CFAI-AFM,[21] Many methods to determination of the samples can be coupled with AFM in future because are depended in the precipitation process,

adsorbent, or on turbidimetry method such as: UV-Vis-spectrophotometry [22] CFIA- NAG-4SX3-3D, [23] UV sunlight Photo reactor, [24] and AYAH 5SX4-ST-5D solar CFI, [25–27] Turbidimetry. [28]

Materials and methods

According to the reaction of cyproheptadine-HCl ($C_{21}H_{22}ClN.1.5\ H_2O$-350.9 g.mol^{-1}) (CPH) with 3,5-dinitro salicylic acid (3,5-DNSA-228.12 g.mol^{-1}) ($C_7H_4N_2O_7$) to form a yellow precipitate, a range of CPH concentrations from 0.005 to 40 mM have been prepared via diluted stock solution of CPH 0.05 M (8.7725 g/500 ml) with distil water that will react with 3,5-DNSA 1 mM (0.11406/500 ml), As well as the reaction of loratadine ($C_{22}H_{23}ClN_2O_2$-382.88 g.mol^{-1}) (LOT) with sodium nitroprusside ($C_{22}H_{23}ClN_2O_2$-297.95 g.mol^{-1}) (SNP) to form a white precipitate, a ranges of concentrations of LOT from 0.01 to 25 mM have been prepared via diluted the stock solution of LOT 0.03M (5.7432 g/500 ml) that will react with SNP 0.8 mM (0.1192/500 ml). The AFM study begins with the synthesis of precipitate coupled with CFIA and the homemade NAG-4(sources) ×3 with three solar cell Analyzer NAG-4SX3-3D analyzer.

Methodology – AFM to study of surface morphology of precipitated ions using flow injection analysis (FIA)-atomic force microscopy (AFM)

The AFM study begins with the synthesis of precipitate coupled with CFIA and the homemade NAG-4(sources)x3 with three solar cell Analyzer NAG-4SX3-3D analyzer, [21,29] which is created by the reaction of drugs cyproheptadine hydrochloride with 3,5-dinitro salicylic acid and loratadine with sodium nitroprusside, and the collecting of samples for analysis. Sampling is critical since it represents the general concept of the kind of precipitate generated. The precipitate is collected while the scatter plot is running; it will be used to construct the calibration graphs. This produces precipitate with varying grain characteristics as a result of varied concentration, which accurately represents the whole precipitate generated. Low, medium, and high concentrations represent the various phases of precipitate formation and crystal development, which vary depending on the kind of precipitate created. The excess reagent needed to finish the reaction and create the analyte precipitate is removed from the precipitation by washing it with distilled water. Fig. 3 shows a manifold device of two lines was used. First line is the carrier line stream (distilled water) that will take and introduce the sample loop segment into the reaction stream then combined with the second line of precipitating agent at a Y-junction that will initiate the formation of precipitate. [4,30] Scheme 1 shows the proposed mechanism of reaction for two drugs.

Two directions are used in the sampling process that need to be followed: to separate the solution from the precipitate, an arbitrary reactant concentration is first employed, followed by the production of a sufficient amount of precipitate on the filter paper placed within the funnel. We will get a consistent, homogenous precipitate feed from this collection. Second, using the same configuration, the precipitate is collected during the scatter depicted calibration

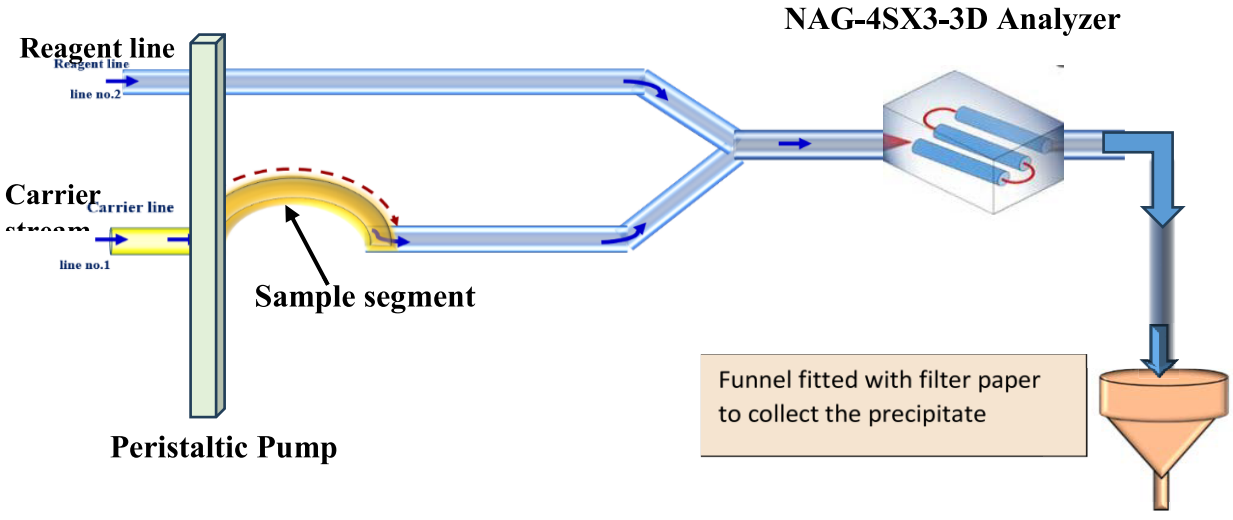

Fig. 3. The flow injection manifold to measure the reaction product of chosen reactant to generate a precipitate, followed by on-line filtration of the reaction product waste product.

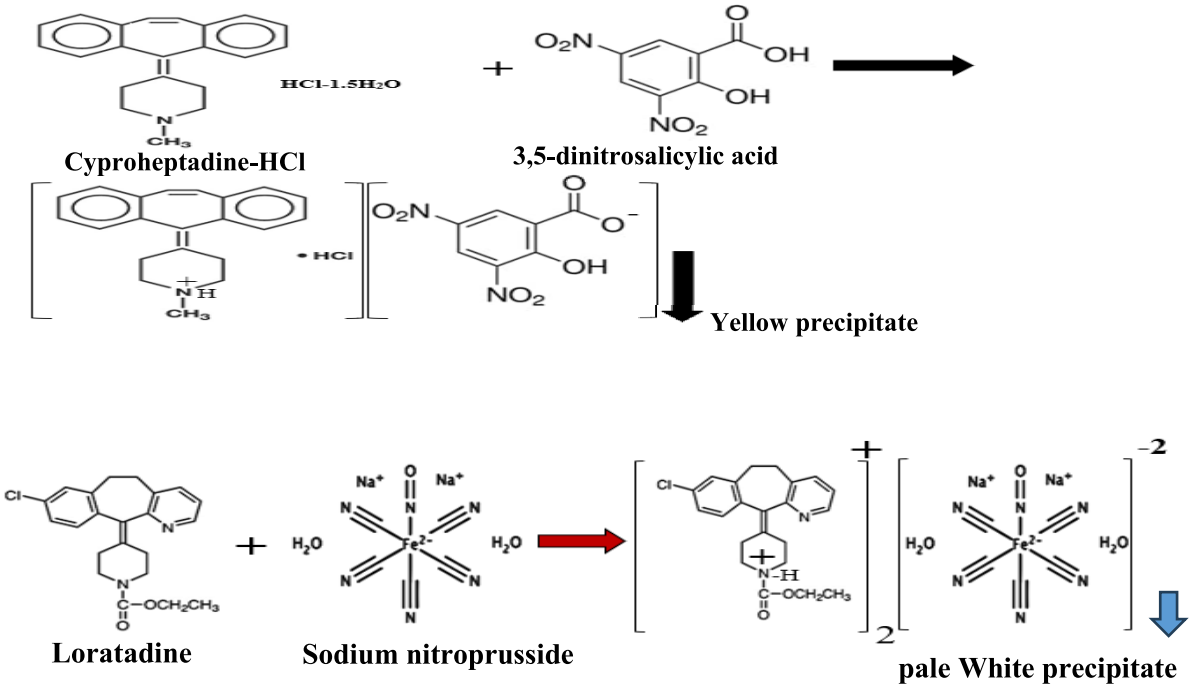

Scheme 1. Proposed reaction for two drugs.

graph build-up. Given that these samples should be regarded as random, low, medium, and high concentrations should all be collected (or at least reproduced for n=3 measurement). Ultimately, it is simply a few milligrams of the same precipitate, sufficient for all the analysis to be completed, but it also necessitates varying structure creation. The excess reagent and other mother liquid chemical that were used to wash the precipitate that had developed on the funnel during the sample process are removed from the funnel. When the filter paper is dry, it is gently sealed and left overnight to prevent any grit. The sample is prepared for atomic force microscopy contour screening. AFM did not assess the reactant of the predicted reaction because of the distinct population and cannot be connected with the precipitate as fineness, i.e., the grain size would be completely different from the precipitate achieved due of the development strategy. Tapping mode was used in the study conducted from (Naio-AFM) for the precipitated.

Results and discussion

Detailed investigation of parameters-model study of formed reactant product (formed precipitate)

Using obtained data parameters for drug

For the experimental preforming of the current methodology adapted in this research work, two samples of nano materials were employed including: sample 1(Cyproheptadine hydrochloride precipitation with 3, 5-dinitro salicylic acid) and sample 2 (Loratadine precipitation with Sodium nitroprusside). All the experiments were conducted using AFM system.

Calculation based on surface area

Sample 1 of cyproheptadine hydrochloride + 3, 5-dinitro salicylic acid. Scanned surface area of rectangle = length × width = 4531 × 4531 nm = 20529961 nm^2.

Since average granule diameter = 96.73 nm, Therefore the surface area for a single granule $\pi(D_{nm})^2$ = 3.14 × $(96.73)^2$ = 29380.015706 nm^2 and for 152 granules it's equal to 152 × 29380.015 nm^2 = 4465762.38731 nm^2

Extra of surface area: 20529961 nm^2 − 4465762.38731 nm^2 = 16064198.61 nm^2

The number of granules on the empty surface area = 16064198.61 nm^2/29380.015706 nm^2 = 546.7729757 granules ≈547 granules

Or: Based that the granules are spheres; therefore, the total surface scanned can take 20529961 nm^2/29380.015706 nm^2 = 698.772975666 spheres ≈699 granules.

So, 698.772975666 − 152 → 546.7762975666 ≈547 granules

Table 1. Distribution of granules size and number of particles of cyproheptadine hydrochloride + 3.5-dinitro salicylic acid.

Parameters	Number of particles	Projected area Mean	Mean diameter [Mean]
Unit Projected Area	152nm^2	nm^2	nm ’
Small	128	8073	66.10
Medium	21	67557	241.5
Large	3	201886	389.8

Therefore, the surface is capable in taking ≈547 granule (i.e., additional layers which is approximately four layers, based on: the number of granules by scanned the instrument = 152 granules.

So, Number of layers = 547/152 = 3.5986842 ≈4 layer.

According to Avogadro's no. 6.02 × 1023 Each mole of material will contain 6.02 × 10^{23} (This is a number only).

Now since there are 699 granules

699/6.02 × 10^{23} = 1.161129568 × 10^{-21} mol = 1.161129568 × 10^{-12} nmol.

Now to determine that the concentration of particpate for each granule (one grain) will be equivalent: 1.161129568 × 10^{-12} nmol/699 = 1.66 × 10^{-15} nmol/granule

Calculation based on volume of scanned by the instrument is:

4531nm × 4531 mm × 63.7 nm = 1307758516 nm^3

Volume of a single granule $\pi/6$ D^3 = 3.14/6 × (96.73)^3 = 473654.819873 nm^3 and for 152 granules = 152 × 473654.819873 nm^3 = 71995532.61 nm^3

Number of granules based on volume number of granules = total scanned volume/volume of single granule 1307758516 nm^3/473654.819873 nm^3 = 2760.994845 granules based on calculated scanned volume 2760.994845 − 152 = 2608.994845 ≈2609 granules the structure can be accommodate.

Based in surface area	Based on volume
547/152	2609/152
4 layers	17 layers

Table 1 shows the distribution of particles based on the variable of diameters, and observed that the number of small particles = 128 compared to the large particles = 3, while Fig. 4. shows the first growth of particulate and then growth for the remainder, followed by the inability to grow due to that the precipitate is collected at different size: small, medium and large.

Fig. 5 shows the low heights of crystal growth which equal to = 8.752(mean height), which is likely to be attributed to the agglomeration of small crystals together in some location, leaving other empty.

Sample 2: Loratadine + Sodium nitroprusside.

Granule diameter = 88.87 nm

Number of granules = 434

Surface area of a single granule assumption again is made that the granule are a spherical in shapes the surface area for a single granule = $\pi(D_{nm})^2$

= 3.14 × (88.87)^2 = 24799.333466 nm^2

surface area of total 434 granules = 434 × 24799.333466 nm^2 = 10762910.72 nm^2

scanned surface area of scanned area by the instrument

4540 nm × 4540 nm = 20611600 nm^2

Extra of surface area: 20611600 nm^2 − 10762910.72 nm^2 = 9848689.276 nm^2

– The number of granules on the empty surface area

9848689.276 nm^2/24799.333466 nm^2 = 397.1352412 granules ≅ 397 granules

Or:

Based on the total surface scanned can take and surface area of single granule, means:

20611600 nm^2/24799.333466 nm^2 = 831.1352413 spheres ≈ 831 granules

831.1352413 − 434 → 397.1352413 ≅ 397 granules

Therefore, the surface is capable in taking ≈ **397** granule (i.e., no additional layers as follow:

The number of granules by scanned the instrument = 434 granules

So, number of layers = 397/434 = 0.9147465 ≈ one layer

On this basis, there is a possibility from scanned surface area (semi filled) to accommodate 397 granules and there is no need to form a second layer, So, 397 granules are not far away from 434 granules.

Or: approximately semi negligible which means that the calculation was not successful in choosing the area to do the measurements, So, it will depend on the volume calculation (below section).

According to Avogadro's no. 6.02 × 10^{23} Each mole of material will contain 6.02 × 10^{23} (This is a number only)

– Now since there are 699 granules.

831/6.02 × 10^{23} → 1.380398671 × 10^{-21} mol → = 1.380398671 × 10^{-12} nmol

Now to determine that the concentration of particpate for each granule (one grain) will be equivalent: 1.161129568 × 10^{-12} nmol/831 → 1.66 × 10^{-15} nmol/granule.

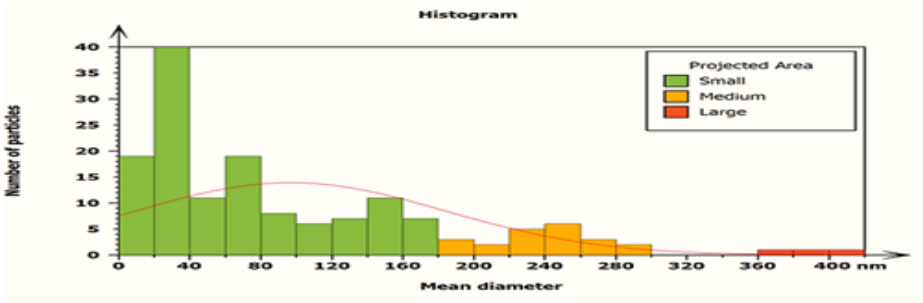

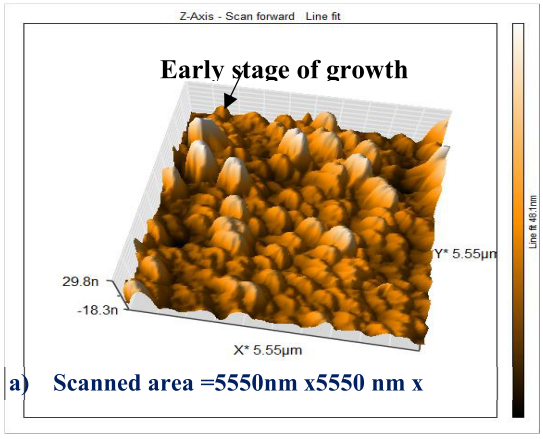

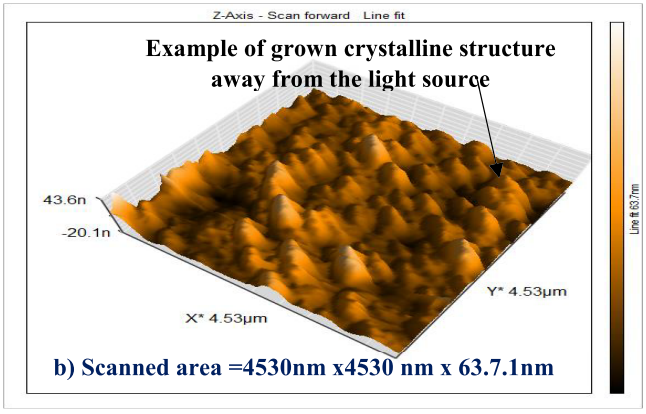

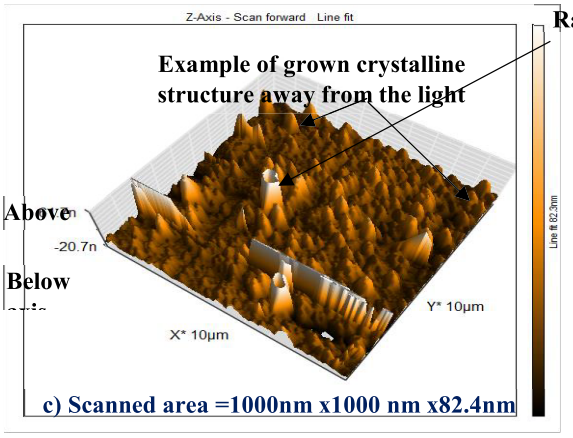

Fig. 4. 3D-Closure topographic view of grown stages of granules formation at variable depth.

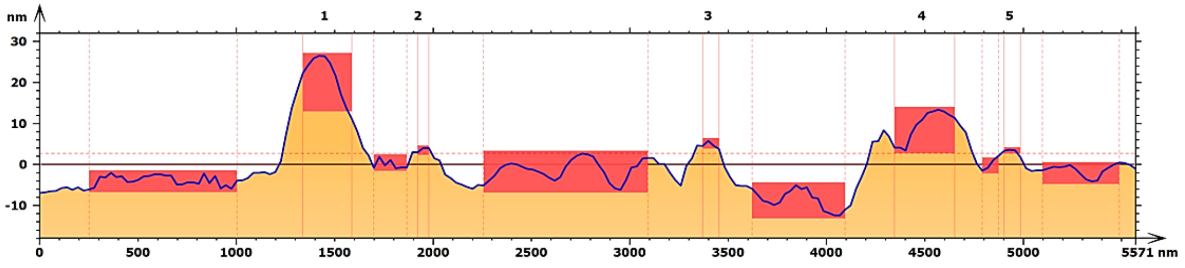

Parameters	Unit	Mean	Min	Max	Step 1	Step 2	Step 3	Step 4	Step 5
Width	nm	156.0	55.71	306.4	250.7	55.71	83.56	306.4	83.56
Maximum height	nm	10.64	3.546	26.49	26.49	3.990	5.783	13.39	3.546
Mean height	**nm**	**8.752**	3.441	22.48	22.48	3.502	4.934	9.402	3.441

Fig. 5. Particle analysis - Threshold detection of crystal growth for cyproheptadine hydrochloride + 3.5-dinitro salicylic acid precipitates and mean height of 8.752 in the table.

– Calculation based on volume of scanned by the instrument is:

Volume of a single granule $= \pi/6\ D^3 \rightarrow$

$3.14/6 \times (88.87\ nm)^3 = 367319.460853\ nm^3$

Therefore, the volume of 434 granule: Number of granules x volume of single granule the volume of 434 granule: $367319.460853\ nm^3 \times 434 = 159416646.01\ nm^3$

The volume that was scanned: Length(nm) × Width(nm) × Depth(nm)

$4540\ nm \times 4540\ nm \times 113\ nm = 2329110800\ nm^3$

Number of granules based on that they are sphere

$2329110800\ nm^3/367319.460853\ nm^3 = 6340.831346 \approx 6341$

While the granules number 434

Therefore, the difference $6341 - 434 = 5906.83$ granules

$$\frac{available\ space}{scanned\ space} : \frac{5906.83}{434} \qquad \frac{397}{434}$$

Layer $\rightarrow 13.6 \approx 14$ layer $0.9147465 \approx$ one layer

This variation is due to that the given granule diameter is constant while in fact it is not, let us take an example a granule of diameter of 100 nm and other of 70 nm:

$\pi/6 \times (100)^3 = 523333.333\ nm^3$ without pressed (no deform ate)

$\pi/6 \times (70)^3 = 179503.333\ nm^3$ deformed.

The difference $\pi/6(100)^3 - \pi/6 * (70)^3 = 343829.99966\ nm^3$

Therefore $523333.333/367319.460853 = 1.45 \approx 2$

$179503.333/367319.460853 = 0.48868 \approx 0.5$

$343829.99966/367319.460853 = 0.93605 \approx 1$

This value of $0.9147465 \approx$ one layer means that a longitudinal column form is build up on one layer that is the originally formed layer. i.e., that is not necessary to cover the whole formed first layer, which gives an indication of the formed crystal structure. This is illustrated in the Fig. 6 below:

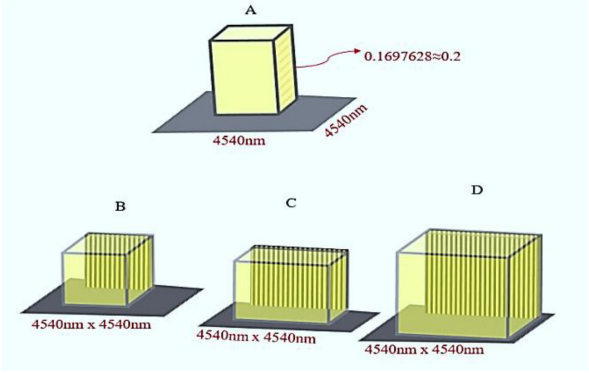

Fig. 6. An approximate imaginary expectation of formed crystal structure on one layer.

*The calculation of standard spherical diameter will be giving us a larger volume from reality i.e., that might give us values approaches e.g. 0.5- 2 as in the previous example for a granule with a diameter of 100nm and an equivalent of two granule. While if the granule were pressed in all directions due to its structure and its diameter become 70nm. The value of granule approaches zero value as its reaches 0.5, and this definitely dose not reach even part of the granule volume, it is quite difficult that the surface area and the volume cannot be considered to be correct.

*All calculations lead to the same conclusion which indicates that the theoretical calculation is far away from the reality and thus due of what the granules suffers from exerted pressure that cause; and cannot be assumed better than that as if it is assumed a cylinder (irregular dimensions) and if it is assumed a cone or other shapes. It will reach that the best choice is the sphere and it might be compact from one side in addition to the base of sampling plate thus giving, oval shape and will never reach to a better result therefore it is better to remain in the form of a sphere.

Fig. 7 and the related table attached to it and Fig. 8 show, the particulates are distribution on surface contour in not homogeneous and this is identical to the above calculation which show, there are empty space location unoccupied with particulate, and area occupied where the particulates are present in the form of agglomeration a bulky with variable heights Fig. 9, and the particles are arranged in layers so that, the small size is at the top and the large at the base of the response.

The discussion of atomic force microscopy results via the formation of solid particulate precipitate with different precipitating agent for determination of drugs, following was noted:

– The $S_{sk} = 15.02$ (skewness) which is a positive value which means the skewness is toward the second quarter. While the value $S_{ku} = 283.2$ (kurtosis) represent the high purity away from the faulty ends (platykurtic). Therefore, looking for high purity i.e., looking for high value of skewness and high values of kurtosis $S_{sk} = 15.02$ meaning the distribution towards a higher value i.e., that toward to the small particles. while $S_{ku} = 283.$, it means a regular and high purity of drug, this depends on active ingredient forming the main drug of cyproheptadine hydrochloride.

While for loratadine the value of $S_{SK} = 0.9325$ which is positive i.e., that skewness in the crystalline form with accepted purity of $S_{ku} = 3.670$ which is regarded as acceptable purity if it is required to prepare derivative of a drug for this compound after studying the medical properties for the product.

– **Mean peak Curvature** for **Cyproheptadine - 3.5-dinitro salicylic acid** precipitate (0.1037), it was 11 time more than **Loratadine- sodium nitroprusside** precipitate (0.009135), i.e., It was

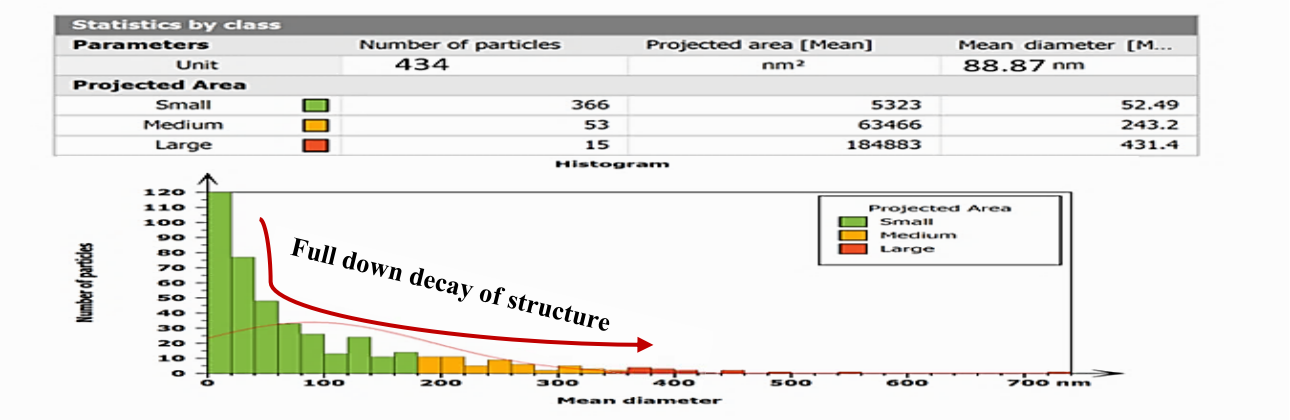

Fig. 7. Projected area distribution showing positive skewness i.e., toward formation of small granules of Loratadine + Sodium nitroprusside with number of particles and mean.

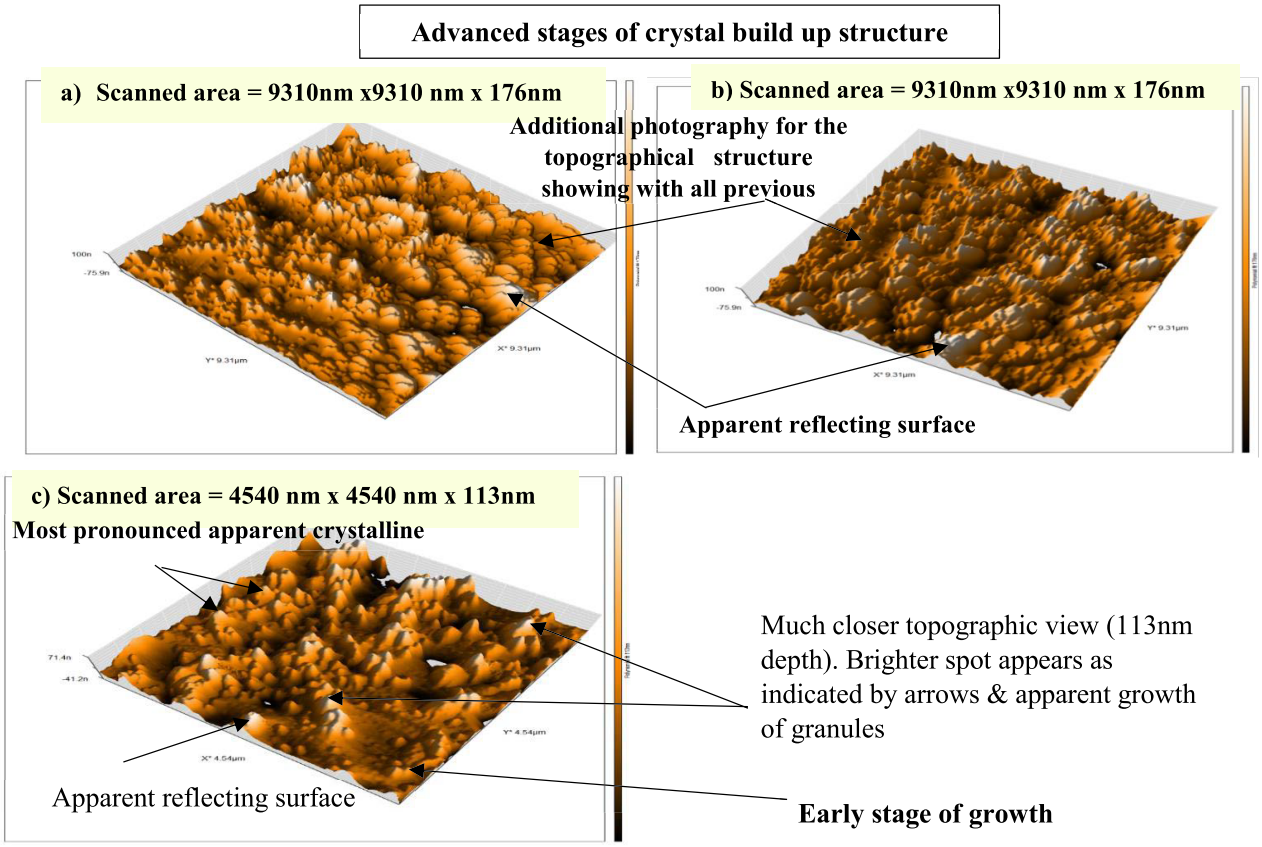

Fig. 8. 3D photograph of crystal growing of Loratadine + Sodium nitroprusside precipitate showing stage of crystal growth at variable depth & much accelerated crystal growth.

0.1037/0.009135 = 11.351943076 which is equivalent to = 11 times,this indicates that the metal ion precipitation reaction does not show any sign of curvature while drug precipitation shows a curvature at the peak which might be a good indication of distinguishing between these two groups i.e., the metal ions or the drugs to more or less extent.

– Maximum five points peak height with 5% pruning equal to 508.2nm while ten-point height at 5% pruning the instrument was not able to detect and measure it might be due to measuring of calibration graph precipitation formation. While density of peak for an area of square nanometer equal to 2.2 $\times$ 10^{-7} with 5% pruning i.e., 2.2 $\times$ 10^{-7} $\times$ $10^{7}/10^{7}$

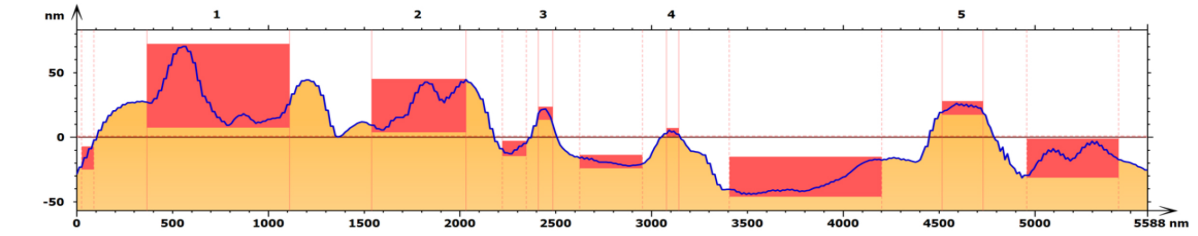

Parameters	Unit	Mean	Min	Max	Step 1	Step 2	Step 3	Step 4	Step 5
Width	nm	317.9	63.07	744.3	744.3	492.0	75.69	63.07	214.5
Maximum height	nm	33.32	5.322	70.29	70.29	43.12	21.78	5.322	26.09
Mean height	**nm**	**20.40**	3.803	29.62	29.62	25.59	19.56	3.803	23.43

Fig. 9. Particle analysis - Threshold detection of crystal growth of Loratadine + Sodium nitroprusside precipitate showing variable height of response.

Table 2. Measurements by AFM of cyproheptadine hydrochloride & Loratadine.

Cyproheptadine hydrochloride			
Spd	2.2e-07 1/nm^2	Pruning = 5%	Density of peaks
Spc	0.1037 1/nm	Pruning = 5%	Arithmetic mean peak curvature
S10z	****	Pruning = 5%	Ten points heights
S5p	508.2 nm	Pruning = 5%	Five points peak height
warning	S10z: Not enough pits were found		
Loratadine			
Spd	6.249e-06 1/nm^2	Pruning = 5%	Density of peaks
Spc	0.009135 1/nm	Pruning = 5%	Arithmetic mean peak curvature
S10z	142.4 nm	Pruning = 5%	Ten points heights
S5p	96.35 nm	Pruning = 5%	Five points peak height

i.e., that 2.2 granules will occupy (1000000) nm^2 Table 2.

Not enough pits were found during measurements which might be due to compactness at lower levels of 4 layers based on the surface area at 152 granules as shown in Table 3 in which the values of mean diameter of granules size based on broad size distribution as small, medium, and large distribution.

Tables 2 to 4 in the case of cyproheptadine hydrochloride, the number of particles = 152, and the particles of small sizes are more than particles of medium and large size. Small particles are compact with each other on the ground layer, as indicated by the value of angle = 0.4199 corresponding to the value of Texture direction = 0.0007329 with the presence of some crystal growth in the form of layer in some location of contour at value of maximum height = 687.2nm, and distributed over faraway location indicated by the value of Dominant spatial wavelength = 70.78 nm. So it was only seen the five points peak height = 508.2 nm, and the tip could not give the value of ten points heights, due to the surface was compacted with small granules so, the depth reached by the tip, maximum pit depth = 23.58 nm, Fig. 10.

In the case of Loratadine, and following up the results in Tables 2 and 3, the number of granules 434 of small size are more compared to the medium and large size, therefore, crystal growth was obtained in

Table 3. The projected area and distribution of granules based on variable of size by AFM of cyproheptadine hydrochloride & Loratadine.

Parameters	Number of particles	Projected area [Mean]	Mean diameter [Mean]
Cyproheptadine hydrochloride			
Unit	nm^2	nm^2	nm
Projected Area			
Small	128	8073	66.10
Medium	21	67557	241.5
Large	3	201886	389.8
Loratadine			
Small	366	5323	52.49
Medium	53	63466	243.2
Large	15	184883	431.4

Table 4. Measurements of dominant spatial wavelength and texture direction of cyproheptadine hydrochloride & Loratadine.

Cyproheptadine hydrochloride			
Sal	36.17 nm	S = 0.2	Autocorrelation length
Str	0.01285 nm	S=0.2	Texture-aspect ratio
Std	0.0007329°	reference angle =0	Texture direction
Ssw	70.78 nm		Dominant spatial wavelength
Loratadine			
Sal	309.9 nm	S=0.2	Autocorrelation length
Str	0.8463 nm	S=0.2	Texture-aspect ratio
Std	177.0°	reference angle = 0	Texture direction
Ssw	19.30 nm		Dominant spatial wavelength

Maximum height = 153.5 nm with Texture direction with reference zero is 89.676 which is equivalent to 177 and distribution in the form of compact clusters throughout the counter that was scanned, so the dominant spatial wavelength = 19.3 nm appeared short and high frequencies, and this indicates that the peak heights resulting from the crystal growth are adjacent to each other with the presence of some unoccupied surface, through which the tip was able to reach at maximum pit depth = 49.03 nm to measure each of Ten points heights= 142.4 nm and Five points peak height = 46.35 nm, Fig. 10.

The below values of granules number Table 5. based on broad size distribution as small, medium, and large distribution. which does not specify that the small or median or the large one of the same

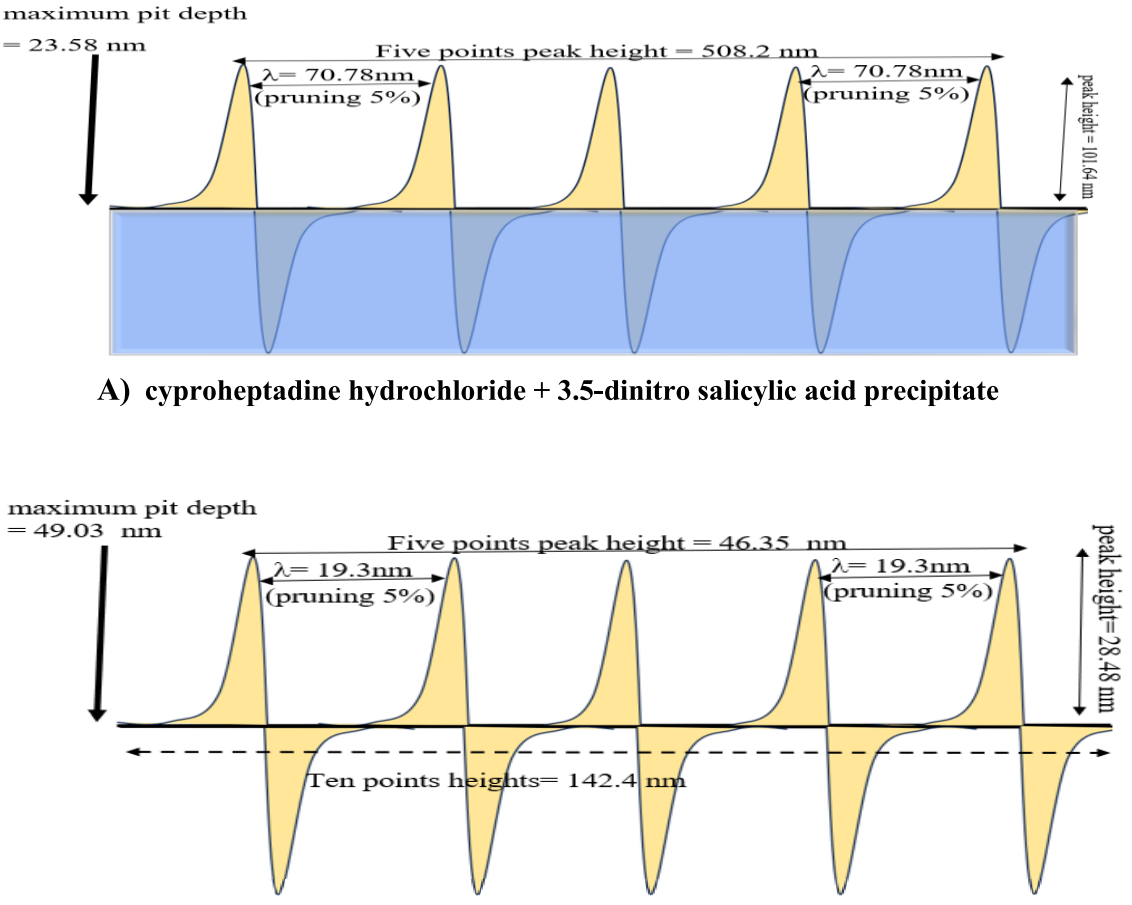

Fig. 10. Showing Ten points heights and Five points peak height of A) cyproheptadine hydrochloride + 3.5-dinitro salicylic acid precipitate B) Loratadine + Sodium nitroprusside precipitate at variable depth.

Table 5. Shows the number of granules of different species of drugs (cyproheptadine hydrochloride & Loratadine).

Type of species	Loratadine	cyproheptadine
Small	366	128
Medium	53	21
Large	15	3
granules number	434	152

dimensions which is not at all due to different time of precipitation proceeding.

• **Since the samples chosen are randomly selected therefore there is no correlation.**

Discussion

It can be noticed that cobalt ion precipitate was taken into little but more detected than the other items in this study. Actually, another version for cobalt ion was written but it was left a side for future study, for example the rapid growth of granules starting from molecular ion, nucleus, particulate and finally granule. From scanned sample specie man showing buildup crystals or granules. From this study, it was noted and a clear indication of build-up of small granules within less than 100 nm which is proves that they are nano particles by tapping mode scanning by Naio-AFM. Taping mode was used in the (Naio-AFM), Abbot – five stone curve or bearing area curve (BAC) which describes the surface texture of an object. The curve can be found from, a profile trace drawing lines parallel to the datum and measuring the fraction of the lies within the profile.

Atomic Force Microscopy is a good tool that will deals with the surface of formed solid precipitate formed in this study. From the above listed study which was dealt with the formation of color precipitated reaction products it was released that all properties of the AFM to give a kind of formed precipitate. This will lead for further investigation when choosing the formation of a certain required product. Restriction of this study with the used of four species does not necessitate that this is the limitation the use of AFM for further future studies.

Conclusion

The precipitate particles generated by the reaction of Cyproheptadine-HCl with 3,5-DNSA, resulting in a yellow precipitate, and the reaction of Loratadine with SNP, resulting in a white precipitate, were examined using CFA and AFM. Upon observation, it is evident that subtracting the area of the scanned surface by AFM from the total surface area of the granules yields either positive or negative findings. If the result of the subtraction is positive, it indicates that there is space for additional granules to form. This is because the concentration of newly formed granules would fill the initial layers on the surface. This can only occur when the reactant concentrations are low, specifically in the lower part of the scatter plot. If the data (subtraction values) are negative, it indicates that there will be no space available at the initial ground monolayer.

Monolayers result in the creation of a subsequent monolayer.

Finally, it can be inferred that a further study should be carried out and what were presented here was the start. A systematic series trend should be done i.e., more than one or two metal ions with the same precipitant and this could be a research project at M.Sc. level or Ph.D. level where a real detailed study can be achieved.

Acknowledgment

Our sincere appreciation goes out to Professor Issam M.A. Shakir for his invaluable counsel, insightful observations, and encouragement.

Authors' declaration

- Conflicts of Interest: None.
- We hereby confirm that all the Figures and Tables in the manuscript are ours. Furthermore, any Figures and images, that are not ours, have been included with the necessary permission for republication, which is attached to the manuscript.
- No animal studies are present in the manuscript.
- No human studies are present in the manuscript.
- Ethical Clearance: The project was approved by the local ethical committee at University of Baghdad.

Author's contribution

B S M and N S T, contributed to the design and implementation of the research, to the analysis of the results and to the writing of the manuscript.

References

1. Mezaal EN, Sadiq KA, Karim TAA. A Review using continuous flow injection analysis technique in the determination of several drugs. IHJPAS. 2024;37(1);221–235. https://doi.org/10.30526/37.1.3182.

2. Sagmeister P, Lebl R, Castillo I, Rehrl J, Kruisz J, Sipek M, *et al.* Advanced real-time process analytics for multistep synthesis in continuous flow. Angew Chem Int Ed Engl. 2021;60(15);8139–8148. https://doi.org/10.1002/anie.202016007.
3. AlMasoud N, Bakheit AH, Alshammari MFM, Abdel-Aziz HA, AlRabiah H. Loratadine. Profiles Drug Subst Excip Relat Methodol. 2022;47:55–90. https://doi.org/10.1016/bs.podrm.2021.10.002.
4. Nagham S, Turkey, Bakr Sadiq Mohammed, MA, Shakir I. Determination of Cyproheptadine-Hydrochloride by Precipitation with 3, 5-Dintrosalicylic Acid via the NAG-4SX3-3D Analyzer at 0-180°. Adv J Chem A. 2024;7(3);303–318. https://doi.org/10.48309/ajca.2024.429307.1463.
5. O'Hara V, Cuda S, Kharofa R, Censani M, Conroy R, Browne NT. Clinical review: guide to pharmacological management in pediatric obesity medicine. Obesity Pillars. 2023;6:100066. https://doi.org/10.1016/j.obpill.2023.100066.
6. Binnig G, Quate CF, Gerber C. Atomic force microscope. Phys Rev Lett. 1986;56(9):930. https://doi.org/10.1103/PhysRevLett.56.930.
7. Dai P, Wang S, Taub H, Buckley JE, Ehrlich SN, Larese JZ, *et al.* X-ray-diffraction and scanning-tunneling-microscopy studies of a liquid-crystal film adsorbed on single-crystal graphite. Phys Rev B Condens Matter. 1993;47(12):7401–7407. https://doi.org/10.1103/physrevb.47.7401.
8. Rief M, Gautel M, Oesterhelt F, Fernandez JM, Gaub HE. Reversible unfolding of individual titin immunoglobulin domains by AFM. science. 1997;276(5315):1109–1112. https://doi.org/10.1126/science.276.5315.1109.
9. Schuler B, Liu W, Tkatchenko A, Moll N, Meyer G, Mistry A, *et al.* Adsorption geometry determination of single molecules by atomic force microscopy. Phys Rev Lett. 2013;111(10):106103.
10. Mohn F, Schuler B, Gross L, Meyer G. Different tips for high-resolution atomic force microscopy and scanning tunneling microscopy of single molecules. Appl Phys Lett. 2013;102(7):1–10. https://doi.org/10.1063/1.4793200.
11. Dong L, Li Y. Experimental identification of topography-based artifact phenomenon for micro-/nanoscale thermal characterization of polymeric materials in scanning thermal microscopy. AIP Adv. 2022;12(4):045311. https://doi.org/10.1063/5.0088360.
12. Alunda BO, Lee YJ. Cantilever-based sensors for high speed atomic force microscopy. Sensors (Basel). 2020;20(17):4784. https://doi.org/10.3390/s20174784.
13. Eun JH, Sung SM, Kim MS, Choi BK, Lee JS. Effect of MWCNT content on the mechanical and piezoelectric properties of PVDF nanofibers. Mater Des. 2021;206:109785. https://doi.org/10.1016/j.matdes.2021.109785.
14. Al-Ani A, Jeber J. Development of a nanostructured double-layer coated tablet based on polyethylene glycol/gelatin as a platform for hydrophobic molecules delivery. Egypt J Chem. 2021;64(4):1759–1767. https://doi.org/10.21608/ejchem.2021.52019.3066.
15. Jassim RA, Sando MS, Farhan AM. Protection of Galvanized steel from corrosion in salt media using sulfur nanoparticles. Baghdad Sci J. 2022;19(2):0347–0347. https://doi.org/10.21123/bsj.2022.19.2.0347.
16. Jassim RA, Farhan AM, Ali AM. Corrosion protection study of carbon steel and 316 stainless steel alloys coated by nanoparticles. Baghdad Sci J. 2014;11(1):116–122. https://doi.org/10.21123/bsj.2014.11.1.116-122.
17. Alwash A. The green synthesize of zinc oxide catalyst using pomegranate peels extract for the photocatalytic degradation of methylene blue dye. Baghdad Sci J. 2020;17(3):0787–0787. https://doi.org/10.21123/bsj.2020.17.3.0787.
18. Shakir IM, HFAR. Combined CFA-AFM Analytical approach for precipitation reaction regarding crystal growth building single and multiple monolayers based on surface area calculation with image surface roughness analysis (unseen surface). J Phy Conf Ser. 2021;2063(1):012031. https://doi.org/10.1088/1742-6596/2063/1/012031.
19. Farhan RZ, Ebrahim SE. Preparing nanosilica particles from rice husk using precipitation method. Baghdad Sci J. 2021;18(3):0494–0494. https://doi.org/10.21123/bsj.2021.18.3.0494.
20. Abbas NK, Shanan ZJ, Mohammed TH. Physical properties of Cu doped ZnO nanocrystiline thin films. Baghdad Sci J. 2022;19(1):0217–0217. https://doi.org/10.21123/bsj.2022.19.1.0217.
21. Hameed SF. A novel approach for study of surface morphology & roughness analysis for characterization of precipitation product at a nanoscale level via the reaction of fluconazole with phosphomolybidic acid. Chem Methodol. 2022;6:385–397. https://doi.org/10.22034/chemm.2022.332594.1450.
22. Jobouri AL. Adsorption study of rhodamin b dye on iraqi bentonite and modified bentonite by nano compounds TiO_2, ZnO, Al_2O_3 and sodium dodecyl sulfate. Am J Environ Sci. 2013;9(3):269–279. https://doi.org/10.3844/ajessp.2013.269.279.
23. Bakr Sadiq Mohammed NST. New homemade NAG-4SX3-3D analyzer for quantification of cyproheptadine hydrochloride by its precipitating with calcium hexacyanoferrate Chem Pap. 2023;78(2);1277–1290. https://doi.org/10.1007/s11696-023-03165-9.
24. Abduljabbar AT, Dhahir SA, Abood WM, editors. Furfural Removal from Simulated Wastewater Using ZnO Nanoparticles/H_2O_2 in Solar Photocatalysis Reactor. J Phy Conf Ser. 2021;1818(1):012048. https://doi.org/10.1088/1742-6596/1818/1/012048.
25. Issam MA. Fares S. Abd-Alrazack H. A Novel Semi Automated On-Line Determination of Oxonium Ion Via Precipitation Reaction Using a New Mode of Attenuated Measurement of Incident Light (0–180 o) by AYAH 5SX4-ST-5D Solar CFI Analyser. Iraqi J Sci. 2014;55(4B):1736–1750.
26. Kareem FT, Hammood MK. Determination of the Quantity of Losartan Active Ingredient in the Medication Formulations via Turbidimetric-Flow Injection Technique. Chem Methodol. 2022;6:41–51. https://doi.org/10.22034/chemm.2022.1.4.
27. Yassin OA. New Method for Estimation Mebeverine Hydrochloride Drugs Preparation by a New Analyser: Ayah 6S.X1(WSLEDs)-T.- Two Solar Cells Complied with C.F.I.A. Baghdad Sci J. 2021;18(3):0565. https://doi.org/10.21123/bsj.2021.18.3.0565.
28. Hammood MK, Jeber JN, Muhamad YH. Two Techniques (Spectrophotometric and Turbidimetric) for Determination of Ciprofloxacin HCl in Pharmaceutical Drugs with Comparison between the Techniques. Iraqi J Sci. 2016;57(3A):1620–1628.
29. Shakir IMA, Abd-Alrazack HF, editors. Novel pioneered approach in understanding the gathering between atomic force microscopy with flow injection analysis study at various steps in precipitation reaction methodology. AIP Conf Proc. 2020;2213(1):020068. https://doi.org/10.1063/5.0000098.
30. Turkey NS, Mohammed BS, Shakir IM. A Novel Study in the Determination of Loratadine in Pharmaceutical Samples by Precipitating with 3,5-Dinitrosalicylic Acid Utilizing the NAG_4SX3_3D Analyzer at 0-180o in Conjunction with the Continuous Flow Injection Analysis (CFIA) Technique. Adv J Chem A. 2024;7(3):260–277. https://doi.org/10.48309/ajca.2024.429274.1462.

أستخدام مجهر القوة الذرية مع تحليل حقن التدفق المستمر بأستخام 4NAG مصادر3X مع ثلاثة خلايا شمسية NAG-4SX3-3D محلل لدراسة الشكل السطحي لترسب هيدروكلوريد السيبروهيبتادين واللوراتادين

بكر صادق محمد، نغم شاكر تركي

قسم الكيمياء، كلية العلوم، بغداد، بغداد، العراق .

الخلاصة

الهدف من هذه الدراسة هو وصف مورفولوجيا السطح باستخدام التحليل حقن التدفق المستمر CFIA و مجهر القوى الذرية AFM ومحلل NAG-4SX3-3D محلي الصنع. باستخدام طريقة جديدة لتقدير كلا العقارين من خلال تفاعل كلا العقارين، تهدف الدراسة إلى تحديد معاملات الخشونة والحصول على كمية كافية من الوزن (الراسب الأبيض من اللوراتادين مع نيتروبروسيد الصوديوم والراسب الأصفر من هيدروكلوريد السيبروهيبتادين مع 3،5-دينيترو ساليسيليك حمض) لعينة AFM. الميزة الرئيسية للتقنية المقترحة هي قدرتها على حساب كمية الجسيمات النانوية التي يمكن أن تملأ مساحة السطح الفارغة. بدءًا من الأرض الأولى، تحسب الطبقة الأحادية مساحة السطح الحرة وتحدد تركيز الجسيمات النانوية المشاركة على السطح. ومن ثم يُقترح نظام تدفق ميكروفلويديك لإنتاج جسيمات نانوية بشكل مستمر عن طريق التفاعل الكيميائي بين كواشف الترسيب والمكونات الطبية الفعالة. تسمح آلية التدفق بتوليف الجسيمات النانوية بشكل سلس وخالي من الانسداد. تم فحص وإصلاح كل حالة حقن التدفق الكيميائي والفيزيائي. متوسط أقطار هيدروكلوريد سيبروهيبتادين لمساحة سطح مقطع ممسوح بأبعاد 20529961 نانومتر2 و $1.6601\ x10^{-15}$نانومول/حبة هي 96.73 نانومتر، رقم الحبة 547، مساحة سطح الحبيبة الواحدة 29380.015706 نانومتر^2، وعدد الطبقات 4 ; بالنسبة للوراتادين، يبلغ متوسط الأقطار 88.87 نانومتر، والحبوب رقم 434، والمساحة السطحية لحبيبة واحدة 24799.333466 نانومتر^2، وعدد الطبقات 1 للقسم الممسوح ضوئيًا الذي تبلغ أبعاده 10762910.72 نانومتر^2 و $1.3804\ x10^{-12}$نانومول/حبة.

الكلمات المفتاحية: مجهر القوة الذرية، محللNAG-4SX3-3D، تحليل تدفق الجريان المستمر، سايبروهبتادين هيدروكلورايد، لوراتدين